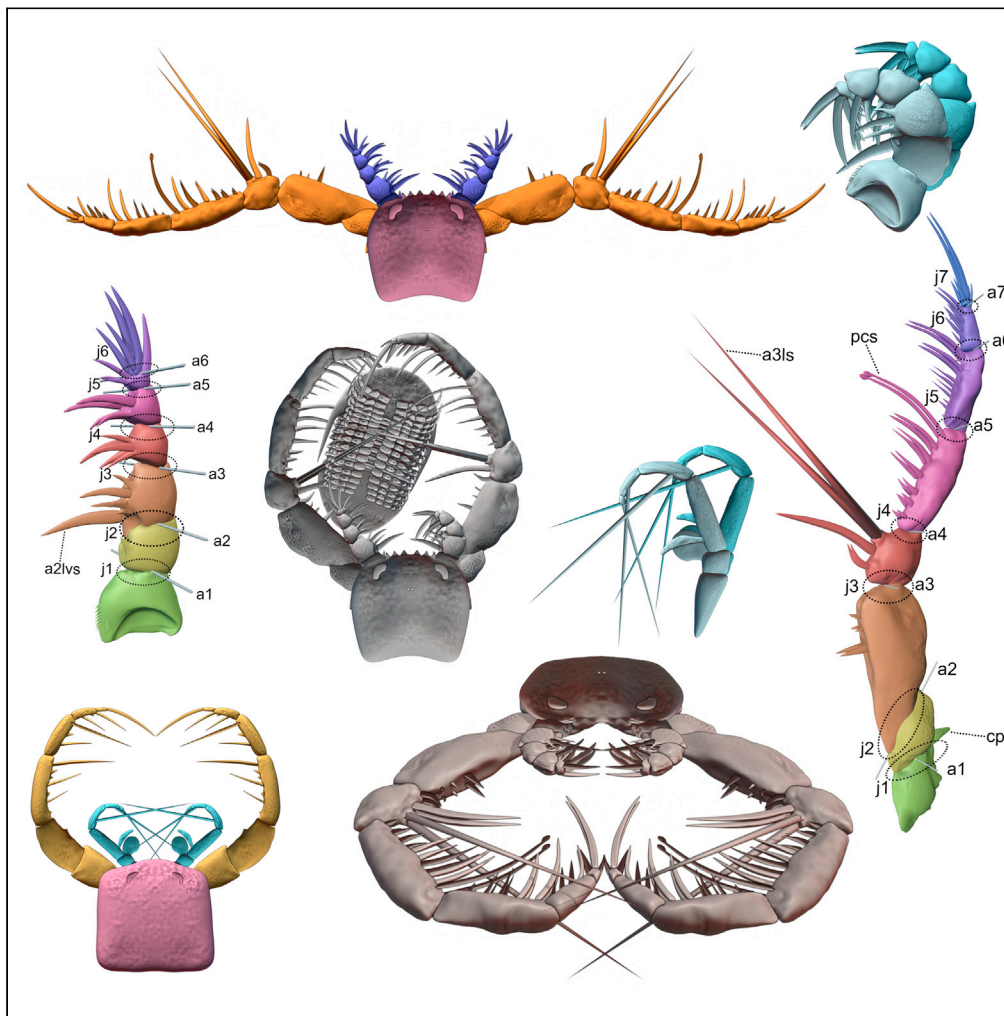


Article

Spines and baskets in apex predatory sea scorpions uncover unique feeding strategies using 3D-kinematics



Michel Schmidt,
Roland R. Melzer,
Roy E. Plotnick,
Russell D.C.
Bicknell

m.schmidt30@outlook.de

Highlights

3D models of two eurypterids were designed for applying virtual kinematic analyses

Megalograptus likely used App III to keep prey, while ripping it off with App II

Mixopterus also kept prey with App III, but impaled it with pointed App II

Both showed great ROM of the frontal appendages comparable to whip spiders

Schmidt et al., iScience 25, 103662
January 21, 2022 © 2021 The Author(s).
<https://doi.org/10.1016/j.isci.2021.103662>

Article

Spines and baskets in apex predatory sea scorpions uncover unique feeding strategies using 3D-kinematics

Michel Schmidt,^{1,2,6,*} Roland R. Melzer,^{1,2,3} Roy E. Plotnick,⁴ and Russell D.C. Bicknell⁵

SUMMARY

Megalograptidae and Mixopteridae with elongate, spinose prosomal appendages are unique early Palaeozoic sea scorpions (Eurypterida). These features were presumably used for hunting, an untested hypothesis. Here, we present 3D model-based kinematic range of motion (ROM) analyses of *Megalograptus ohioensis* and *Mixopterus kiaeri* and compare these to modern analogs. This comparison confirms that the eurypterid appendages were likely raptorial, used in grabbing and holding prey for consumption. The *Megalograptus ohioensis* model illustrates notable Appendage III flexibility, indicating hypertrophied spines on Appendage III may have held prey, while Appendage II likely ripped immobilized prey. *Mixopterus kiaeri*, conversely, constructed a capture basket with Appendage III, and impaled prey with Appendage II elongated spines. Thus, megalograptid and mixopterid frontalmost appendages constructed a double basket system prior to moving dismembered prey to the chelicerae. Such 3D kinematic modeling presents a more complete understanding of these peculiar euchelicerates and highlights their possible position within past ecosystems.

INTRODUCTION

Sea scorpions (eurypterids) represent some of the morphologically and ecologically most diverse Paleozoic euchelicerates (Lamsdell and Selden, 2017; Bicknell et al., 2020, 2021b). The group ranged from the Lower Ordovician (Lamsdell et al., 2015) until close to the end Permian (Lamsdell and Selden, 2017). Across this time, the group explored different life modes, including functioning as predators (Waterston, 1964; Selden, 1984; Chlupáč, 1994; Braddy et al., 2008; McCoy et al., 2015; Poschmann et al., 2016; Bicknell and Amati, 2021), scavengers (Waterston, 1979; McCoy et al., 2015; Bicknell et al., 2018b; Hughes and Lamsdell, 2021), and even sweep-feeders (Waterston et al., 1985; Hughes and Lamsdell, 2021). Despite this range of proposed life modes, limited biomechanical or kinematic studies have been presented to support these interpretations (Plotnick, 1985; Plotnick and Baumiller, 1988; Bicknell et al., 2021b). This is striking as eurypterids are occasionally exceptionally well preserved (Holm, 1898; Selden, 1981; Braddy, 2001; Lamsdell et al., 2015; Bicknell and Amati, 2021) with enough anatomical information to permit three-dimensional (3D) reconstructions and modeling. Here, we present advanced reconstructions of *Megalograptus ohioensis* Caster and Kjellesvig-Waering (1955) (Elkhorn Formation, Late Ordovician, Ohio, USA, Megalograptidae) and *Mixopterus kiaeri* Størmer (1934) (Ringerike Group, Late Silurian, Norway, Mixopteridae) prosomal appendages and illustrate kinematic models that uncover facets of feeding within the two genera. These taxa represent examples of eurypterids with raptorial appendages that may have functioned comparably to extant euchelicerates, such as whip spiders (Amblypygi). To test this theory, and further expand the application of 3D kinematics to euchelicerates, we reconstructed the second and third prosomal appendages of both taxa for analysis. We compare the appendage range of motion (ROM) to that of extant whip spiders to provide compelling arguments that these extinct eurypterids were effective predators that may have engaged in distinct modes of attack.

RESULTS

Kinematics in *Megalograptus*

Megalograptus ohioensis Appendage II (Figures 1A, 1B and S1) has podomeres that generally taper distally; most bear stout dorsal and ventral spines, except for large proximal ventral spine on podomere 3 (a2lvs). Appendage II, in general, has limited ROM (Figures 2A, 2C, 2F, and 2G). However, at maximum

¹Bavarian State Collection of Zoology, Bavarian Natural History Collections, Munich, Germany

²Department Biology II, Ludwig-Maximilians-Universität München, Munich, Germany

³GeoBio-Center, Ludwig-Maximilians-Universität München, Munich, Germany

⁴Department of Earth and Environmental Sciences, University of Illinois at Chicago, Chicago, IL, USA

⁵Palaeoscience Research Centre, School of Environmental and Rural Science, University of New England, Armidale, Australia

⁶Lead contact

*Correspondence:

m.schmidt30@outlook.de

<https://doi.org/10.1016/j.isci.2021.103662>



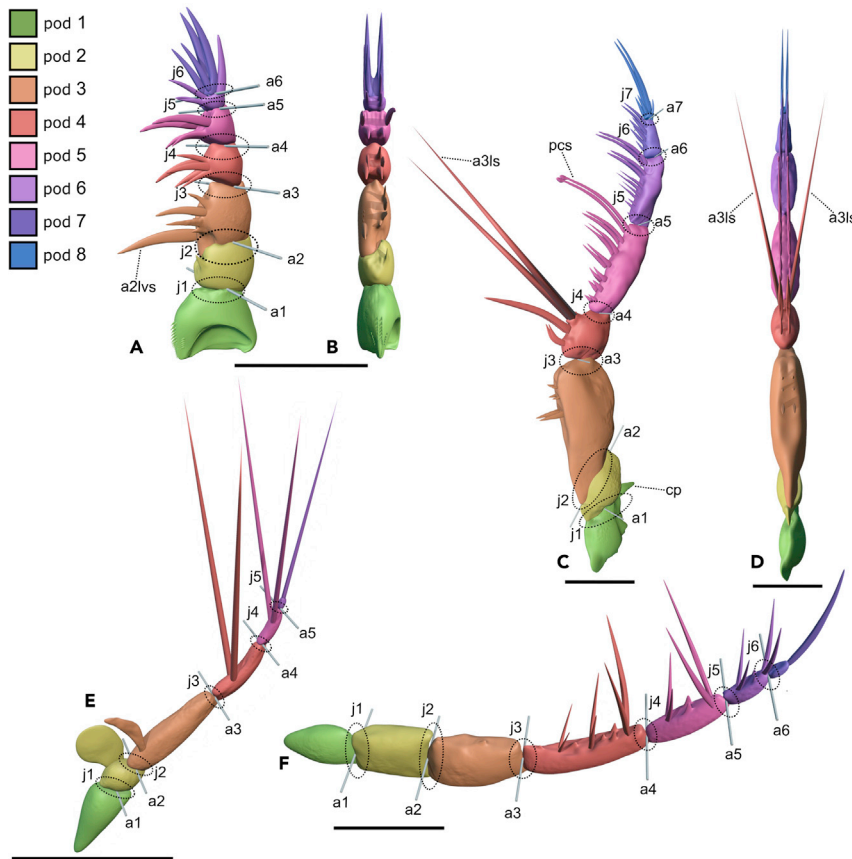


Figure 1. Overview of podomere, joint and joint axes terminology

(A–D) *Megalagraptus ohioensis*. (A) Appendage II, dorsal view. (B) Appendage II, medial view. (C) Appendage III, dorsal view. (D) Appendage III, medial view. (E, F) *Mixopterus kiaeri*. (E) Appendage II, dorsal perspective view. (F) Appendage III, dorsal perspective view. Abbreviations: a1–6: hypothetical joint axes 1–6. a2lvs: Appendage II large ventral spine. a3ls: Appendage III large spine. cp: coxal process. j1–7: joints 1–7. pcs: putative chemosensory structure. pod: podomere. Scale bars: 50 mm.

adduction, the podomere spines interlock (Figures 2C and 2D). The large spine on podomere 3 (a2lvs, Figure 1A and S1) limited anterior-posterior movement (Figure 2D), although it possibly brought prey items close to the inferred position of the chelicerae.

Appendage III (Figures 1C, 1D, and S2) has longer and thinner dorsal and ventral spines. The spine size increases distally on each podomere. Podomere 4 is unique with two distal elongate, hypertrophied spines (a3ls) and podomere 5 has distal spines with blunt, globose tips (pcs). The Appendage III morphology permitted marked posterior-lateral abduction, resulting in large ROM (Figures 2A, 2C, 2F, and 2G). Abduction might have been stopped when the coxal process (cp) collided with the coxa of prosomal Appendage IV. However, this process was also thought to have functioned as an attachment site for muscles (Caster and Kjellesvig-Waering, 1964, p. 321, text Figures 7 and 8). When viewed from above, the vertical joint axis of joint 2 (podomere 2-podomere 3 joint) allowed the entire leg to move dorsally. This movement (elevation and depression) allowed a motion of about 25° of the leg (Table S2). Together, the two appendages formed a spinose basket for prey capture (Figures 2C–2G). The large spines (a3ls) on Appendage III likely trapped prey items, while the stouter spines on Appendage II ripped and tore them for consumption. The function of the blunt spines (pcs) on podomere 5 of Appendage III is unclear, although they may have played a chemo- or mechanosensory role (Caster and Kjellesvig-Waering, 1964, p. 323, also plate 49, Figure 2, text Figure 7 therein).

Kinematics in *Mixopterus*

Mixopterus kiaeri has markedly different appendage morphologies (Figures 1E, 1F, S3, and S4). Appendage II has podomeres of different length (with podomere 3 being the largest) that taper distally,

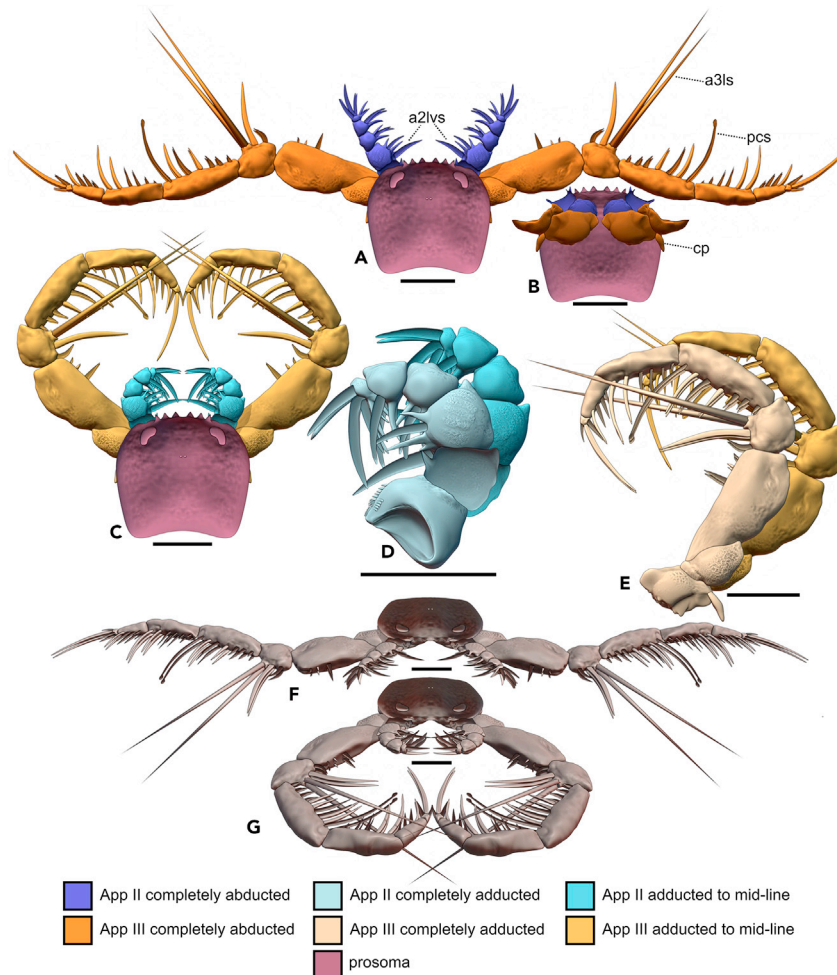


Figure 2. Kinematic models of *Megalograptus ohioensis* raptorial Appendages II and III

(A) Appendages II and III maximally abducted.
 (B) Prosoma showing possible insertion of coxae, ventral view.
 (C) Appendages II and III adducted until points of contact.
 (D) Appendage II maximally adducted (front) and adducted until points of contact (back).
 (E) Appendage III maximally adducted (front) and adducted until points of contact (back).
 (F) Appendages II and III maximally abducted.
 (G) Appendages II and III adducted until points of contact.
 (A, C–E) Dorsal view. (B) Ventral view. (F, G) Anterior perspective view. Abbreviations: a2lvs: Appendage II large ventral spine. a3ls: Appendage III large spine. App II: Appendage II. App III: Appendage III. cp: coxal process. pcs: putative chemosensory structures. Scale bars: 50 mm.

with the terminal podomere tipped with a spine (Figure 1E and S3). Furthermore, podomeres 4 and 5 of Appendage II have elongate spines. At maximum adduction (Figures 3D and 3F), the spines on this appendage reached the chelicerae. The Appendage III has hypertrophied spines on podomeres 4–7. This appendage could also open wide. However, the stout proximal podomeres limited the degree closure when compared to *Me. ohioensis*. These two appendages also produced a large, spinose capture basket (Figures 3C–3F).

Size relations

Taking prosomal width and length measurements of the *Megalograptus ohioensis* and *Mixopterus kiaeri* holotypes as a proxy, we took digital measurements for our models to get comparable metric data (Figure S5 and Table S1).

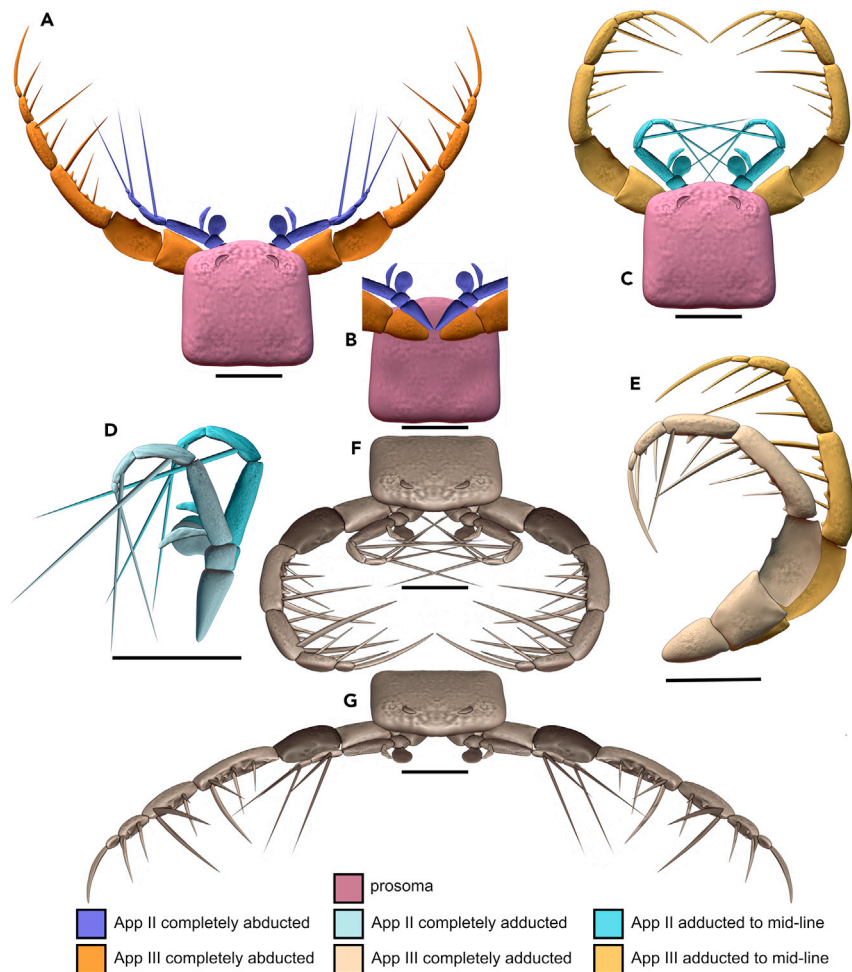


Figure 3. Kinematic models of *Mixopterus kiaeri* raptorial Appendages II and III

(A) Appendages II and III maximally abducted.
 (B) Prosoma showing possible insertion of coxae, ventral view.
 (C) Appendages II and III adducted until points of contact.
 (D) Appendage II maximally adducted (front) and adducted until points of contact (back).
 (E) Appendage III maximally adducted (front) and adducted until points of contact (back).
 (F) Appendages II and III adducted until points of contact.
 (G) Appendages II and III maximally abducted.
 (A, C–E) Dorsal view. (B) Ventral view. (F, G) Anterior perspective view. Abbreviations: App II: Appendage II. App III: Appendage III. Scale bars: 50 mm.

With a rather similar prosomal length (*Megalograptus ohioensis*: 96 mm, *Mixopterus kiaeri*: 93 mm), appendages can be compared on the same scale. When fully abducted, the *Me. ohioensis* model opens its Appendages III up to 765 mm across, while *Mi. kiaeri* was limited to 329 mm. Appendage II can be abducted to 157 mm in *Me. ohioensis*, whereas *Mi. kiaeri* reaches 235 mm, reflecting podomere shape and flexibility (Figures S5A and S5B). When adducted, Appendage III span slightly differs (*Me. ohioensis*: 282 mm, *Mi. kiaeri*: 211 mm). Adduction in Appendage II is rather similar (*Me. ohioensis*: 106 mm, *Mi. kiaeri*: 114 mm; Figure S5C and S5D). Modeled prey size (Figures S5E and S5F) was about 174 mm (trilobite) and 110 mm (anaspid), see discussion.

Range of motion analyses

Comparing the ROM of eurypterid appendages to whip spiders—proposed modern analogs—there are some marked similarities (Figures S6–S8, Table S2). The maximum motion occurs at joint 3, the femur-tibia joint for whip spiders, and the podomere 3–4 joint in eurypterids (Figure S6). Furthermore, the motion of

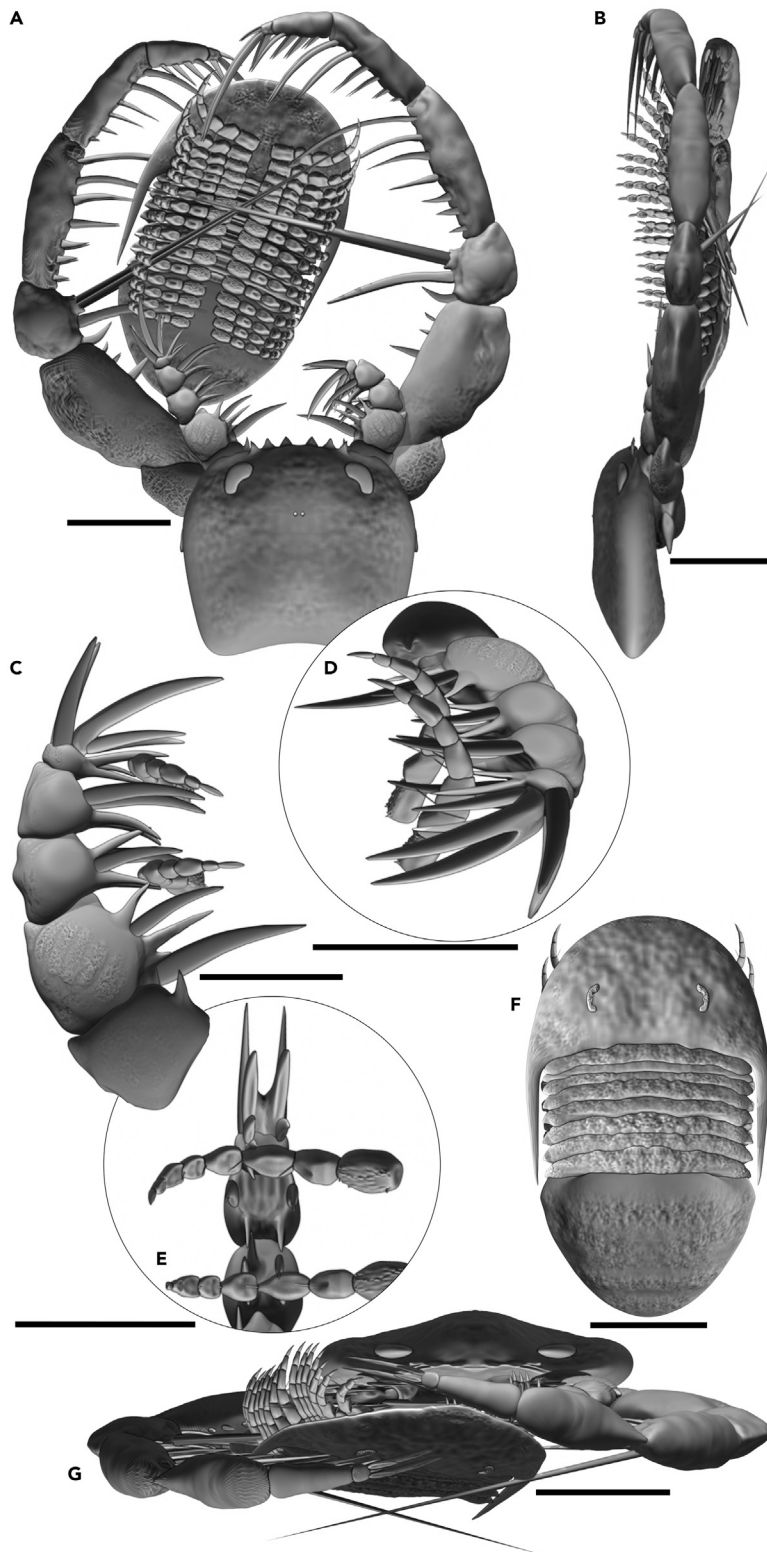


Figure 4. Possible foraging strategy in *Megalagraptus ohioensis*, using Appendage III pair to capture and Appendage II pair to break up prey

Proposed predation on captured freshly molted Ordovician trilobite (*Isotelus*) ventral part upside.

(A) Dorsal view.

Figure 4. Continued

(B) Lateral view.

(G) Anterior view.

(C–E) Single isolated Appendage II with trilobite legs using the scissor-like interlocking function of the medial spines. Coxa not shown.

(C) Dorsal view.

(D) Anterior perspective view.

(E) Medial view.

(F) Trilobite prey model. Dorsal view. Note that trilobite leg models only bear endopodites due to simplicity. Scale bars: (A, B, F): 50 mm. (C–E): 25 mm.

distal podomeres was comparable in both sea scorpions and whip spiders. However, overall eurypterids possibly had lower range of motion at joint 3 than whip spiders (also see [Schmidt et al., 2021b](#); [Figures S7 and S8](#) in this publication).

DISCUSSION

Whip spiders (Amblypygi) are dorso-ventrally flattened, terrestrial euchelicerate ambush predators from the tropics, subtropics, and the Mediterranean ([Harvey, 2003](#); [Weygoldt, 2000, 2002](#)). They bear elongate and spinose raptorial pedipalps ([Santer and Hebets, 2009](#); [Weygoldt, 1996](#)). Select taxa (like our analyzed *Damon medius* and *Heterophrynus elaphus*) form a capture basket to feed on small terrestrial arthropods (see also [Prendini et al., 2005](#); [Garwood et al., 2017](#)). This structure is produced when they adduct distal podomeres such that the entire pedipalps with their spines form a cage ([Figure S8](#)).

Similarities in ROM and capture basket construction between examined eurypterids and whip spiders illustrate that the extinct forms would have captured prey items similarly to whip spiders. Furthermore, the limited motion at joint 3 in the eurypterids is compensated for with the increased podomere count in Appendage III. As such, comparable capture baskets can be produced, albeit slightly less effectively.

Foraging in *Megalograptus*

Megalograptus ohioensis likely seized prey with Appendage III and may have used the podomere 4 hypertrophied spines to hold prey and bring them to chelicerae and the coxal gnathobases with rows of opposing spines. As total length of the hypertrophied spines is not completely known and neither the distal end of the spines is ([Caster and Kjellesvig-Waering, 1964](#), p. 323, also plate 46 Figure 5 therein), we consider it likely that they did not necessarily use those large spines to primarily impale, but constrain prey.

Our proposed foraging strategy in *Megalograptus ohioensis* would have been effective when targeting flat organisms ([Figure 4](#)). *Megalograptus ohioensis* likely employed the interlocking spines morphologies on Appendage II during adduction to break and rip prey and move food to the chelicerae ([Figures 4C–4E](#)). We have modeled *Me. ohioensis* here consuming a possible trilobite prey. The evidence to suggest that *Me. ohioensis* may have consumed trilobites (albeit soft-shelled) is coprolites containing *Isotelus* sp. and eurypterid prosomal fragments associated with *Me. ohioensis* ([Caster and Kjellesvig-Waering, 1964](#), p. 337). However, prey must have been freshly molted. A biomineralized exoskeleton would have damaged the spines, and a fully enrolled, biomineralized trilobite would have broken the capture basket, likely causing damage. Enrollment in trilobites, moreover, was a well-established defense strategy ([Esteve et al., 2011, 2017](#); [Ortega-Hernández et al., 2013](#)). Furthermore, *Me. ohioensis* unlikely had fortified gnathobases like xiphosurids, so it would have been biomechanically incapable of crushing any biomineralized prey ([Bicknell et al., 2018a, b](#); [Bicknell et al., 2021a](#)). Indeed, even when gnathobasic spines in eurypterids are known, they show limited evidence of shell-crushing ability ([Selden, 1981](#); [Bicknell et al., 2018b](#)).

Megalograptus ohioensis may have also consumed pelagic soft-bodied prey such as jellyfish, ctenophores, and other nektobenthic taxa. In the Cincinnati, many other organisms such as graptolites, scolecodonts, or even conodonts occurred and might have been also preyed on ([Meyer and Davis, 2009](#)). [Caster and Kjellesvig-Waering \(1964, p. 337\)](#) further suggested post-coital cannibalism (p. 337). Regardless, *Me. ohioensis* was clearly not a scavenger; this would have made its highly armored frontal appendages superfluous.

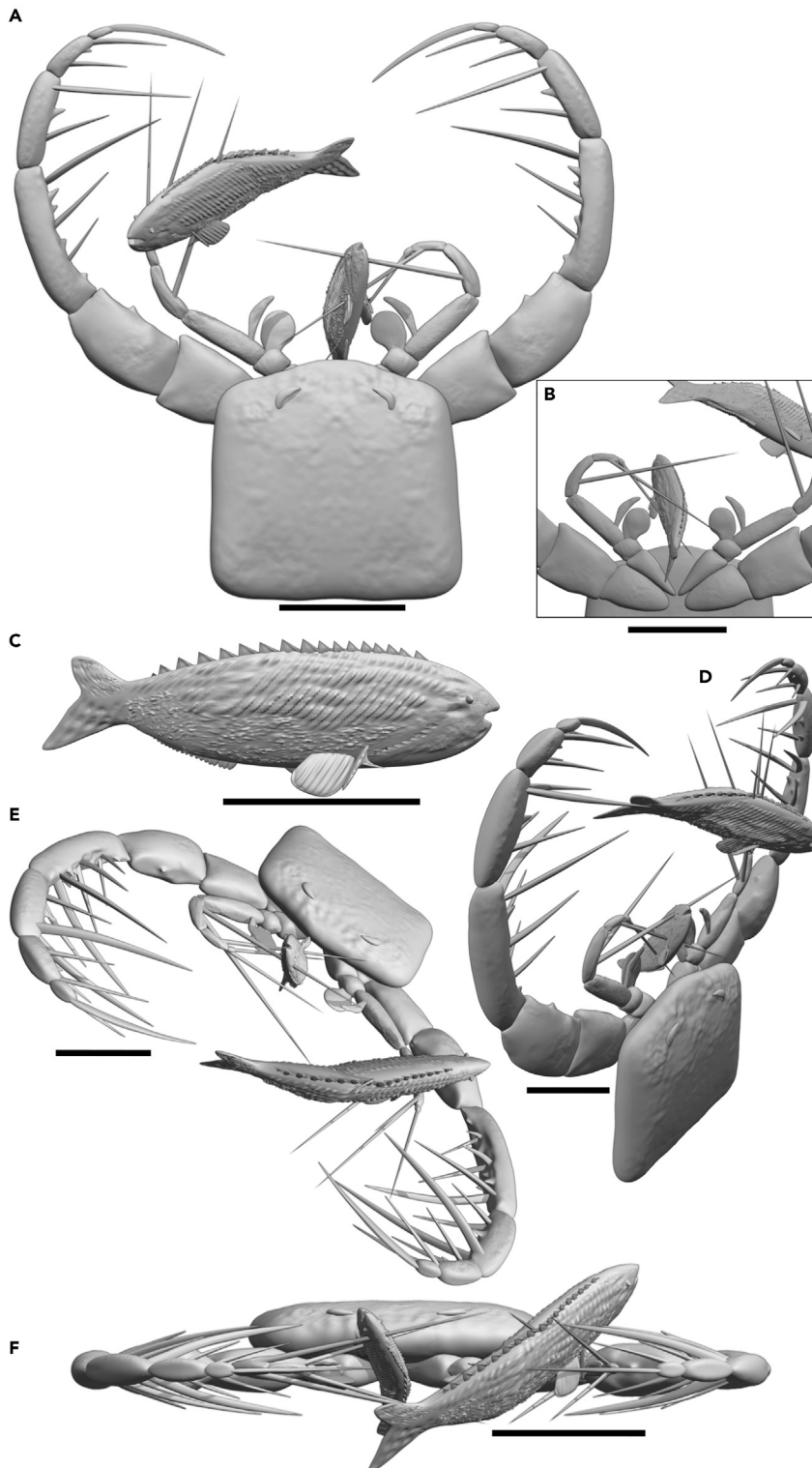


Figure 5. Possible foraging strategy in *Mixopteris kiaeri*, using Appendage III pair to capture prey and get it closer and Appendage II pair to impale prey. Proposed predation on impaled Silurian anaspid agnathan *Rhyncholepis*
(A) Dorsal view.

Figure 5. Continued

- (B) Close-up of right Appendage II getting impaled prey close to the chelicerae (not modeled) below the prosomal shield. Ventral view.
- (C) Anaspid prey model. Lateral view.
- (D) Anterior-dorsal perspective view.
- (E) Anterior perspective view.
- (F) Anterior view. Scale bars: 50 mm.

Foraging in *Mixopterus*

A slightly different feeding strategy is proposed for *Mixopterus kiaeri* (Figure 5). Appendage III has a lower ROM and is less spinous than *Megalograptus ohioensis*, while Appendage II has more elongate spines. These morphologies would have been ideal for impaling prey. The elongated spines are likely to break, so softer prey would have been the primary focus for predation. Appendage III would have created a capture basket to grapple, potentially impale prey and Appendage II would have further immobilized the prey item. Although we modeled *Mi. kiaeri* feeding on an agnathan anaspid fish (*Rhyncholepis* sp.), it could also have preyed on other jawless fish, such as thelodonts and other less heavily armored lower vertebrates, early osteichthyids, jellyfish, or other eurypterids. Niche differentiation in terms of prey may have also played a role, as another species, *Mixopterus multispinosus* from the Pittsford Shale of New York, occurred with no fish biota surrounded (but conodonts), rather likely feeding on phyllocarids or other eurypterids, which were far more abundant (Collette and Plotnick, 2020). This is reflected by the different spinosity of Appendage III in this species (Ruedemann, 1921, plate 1, Figure 3). The heavily armored placoderms, for example, would less likely have been preyed on as they would have damaged the spines.

Sexual dimorphism

Genital appendages are a primary means of differentiating between eurypterid sexes (Størmer and Kjellesvig-Waering, 1969; Tollerton, 1989). However, for both, *Mixopterus* and *Megalograptus*, also intraspecific variability concerning hetero- and homonomous body conditions could have indicated different sexes like given in the trilobite *Paradoxides* (Gozalo et al., 2003).

However, the morphology of frontal appendages may have been sexually selected. Males of select whip spider species possess larger pedipalps than females with sometimes more pronounced spinosity (McArthur et al., 2018; McLean et al., 2019). Given this situation, male megalograptids or mixopterids may have had larger Appendages III, to serve functions like male-male contests.

Another possibility is given if they had developed oversized and thus rather unpractical Appendages III. This handicap in the light of evolutionary biology would have shown females a high level of fitness and would have thus forced their mating success (Zahavi, 1975).

Within the two examined eurypterid taxa there are select appendage morphologies that may have been sexually selected. The globose terminal points from podomere 5 spines of the *Megalograptus ohioensis* Appendage III were unlikely used in prey capture. However, it may have had sensory functions (Caster and Kjellesvig-Waering, 1964, p. 323, also plate 49, Figure 2, text Figure 7 therein) or a possible sexually selected function.

Furthermore, also the telson of *Me. ohioensis* was discussed in playing a role in copulation (Caster and Kjellesvig-Waering, 1964, p. 335).

Sexual selection may have also been established in *Mixopterus kiaeri*. Hanken and Størmer (1975, Figure 10) reconstructed a *Mixopterus* male holding a female from behind (like modern *Limulus*) with prosomal Appendages II and III grasping the opisthosoma of the female and the flat extensions of podomeres 2 and 3 (Figures 1E, 3A–3D, 5A, 5B, and 5C) functioning as a “clasping organ”. This clasping organ was earlier shown and discussed in Ruedemann (1921, p. 10, plate 1, Figure 3D) and Størmer (1934, pp. 49, 50, Figure 20).

Ecological implications

The large frontal appendages of megalograptids and mixopterids may have limited the swimming ability compared to taxa like *Eurypterus* De Kay, 1825 or *Pterygotus* Agassiz, 1849 (Selden, 1981, 1984; Hanken

and Størmer, 1975). In addition, megalograptids and mixopterids bore smaller swimming legs in relation to the body length. This logic can also be extended to consider the telson (Kjellesvig-Waering, 1964; Toller-ton, 1989). Pterygotid species—active, fast-moving predators—have flat paddle-shaped telsons that may have aided in acceleration (Plotnick, 1985; Plotnick and Baumiller, 1988; Selden, 1984). This telson morphology is not observed in *Mixopterus* and *Megalograptus*. *Mixopterus* has a curved, scorpionoid telson (Ruedemann, 1921, plate 1, Figure 5; Størmer, 1934, p. 114) that may have been used in harming prey (Hanken and Størmer, 1975, p. 267, Figure 9D).

Megalograptus, however, possessed a telson unlike any other known eurypterid in having two laterally opposable sickle-like cercal blades, which might have been used in grabbing or even slicing (Caster and Kjellesvig-Waering, 1964, p. 308, text Figures 29, 30).

We assume *Megalograptus ohioensis* and *Mixopterus kiaeri* foraged as ambush predators (like whip spider analogs, but aquatic), slowly swimming over the seafloor, and waiting for prey to cross their way. This would have been more energy-efficient than an actively hunting lifestyle. Thus, appendages bearing strong spines to keep prey would be a benefit. The relatively small forward-facing eyes may also support the interpretation as ambush predators, like the pterygotid *Acutiramus* (McCoy et al., 2015).

Limitations of the study

Kinematic results and ecological implications might be considered regarding several modeling aspects. Megalograptid and mixopterid fossils are always preserved dorsally, or slightly crushed, if preserved laterally. Thus, inflation was inferred from modern euchelicerate appendages. Furthermore, several anatomical details of the fossils like the distal part of the coxa (podomere 1) of Appendage III in *Megalograptus ohioensis* was not preserved according to the original literature (Caster and Kjellesvig-Waering, 1964). In addition, neither total length of the hypertrophied spines on podomere 4 in *Me. ohioensis* nor the angle between them is known. Furthermore, some spines were not preserved as pairs (like the blunt spines on podomere 5 with the bulb-like endpiece; Caster and Kjellesvig-Waering, 1964, p. 323, also plate 49, Figure 2, text Figure 7 therein).

Thus, a different morphological setup than what we modeled might have had impact on the animals' foraging and feeding strategy.

STAR★METHODS

Detailed methods are provided in the online version of this paper and include the following:

- KEY RESOURCES TABLE
- RESOURCE AVAILABILITY
 - Lead contact
 - Materials availability
 - Data and code availability
- EXPERIMENTAL MODELS AND SUBJECT DETAILS
- METHOD DETAILS
 - Modern analogs
 - 3D reconstructions of eurypterids and prey
 - Kinematic marionettes
 - ROM analyses
 - Movement directions
 - Spines
 - Terminology
- QUANTIFICATION AND STATISTICAL ANALYSES

SUPPLEMENTAL INFORMATION

Supplemental information can be found online at <https://doi.org/10.1016/j.isci.2021.103662>.

ACKNOWLEDGMENTS

The authors gratefully acknowledge financial support by Deutsche Forschungsgemeinschaft, Award Number: Me-2683/10-1 (to MS), an Australian Research Council Discovery grant (DP200102005), and a UNE

Postdoctoral Research Fellowship (to RDCB). We also thank Joseph Walkowicz for the photographs in the Supplemental. Finally, we thank the three anonymous reviewers for their comments that greatly improved the direction and scope of this research.

AUTHOR CONTRIBUTIONS

M. Schmidt designed the 3D models, ran the kinematic analyses, and created the figures. R.D.C. Bicknell, R. R. Melzer, and R. Plotnick conceived and supervised the project. M. Schmidt and R.D.C. Bicknell wrote the first draft with input from the other authors. All authors discussed the results and commented on the manuscript.

DECLARATION OF INTERESTS

The authors declare no competing interests.

Received: October 24, 2021

Revised: November 21, 2021

Accepted: December 16, 2021

Published: January 21, 2022

REFERENCES

- Bicknell, R.D.C., and Amati, L. (2021). On the morphospace of eurypterine sea scorpions. *Earth Environ. Sci. Trans. R. Soc. Edinb.* <https://doi.org/10.1017/S175569102100030X>.
- Bicknell, R.D.C., Ledogar, J.A., Wroe, S., Gutzler, B.C., Watson, W.H., III, and Paterson, J.R. (2018a). Computational biomechanical analyses demonstrate similar shell-crushing abilities in modern and ancient arthropods. *Proc. R. Soc. Lond. B: Biol. Sci.* *285*, 20181935.
- Bicknell, R.D.C., Paterson, J.R., Caron, J.-B., and Skovsted, C.B. (2018b). The gnathobasic spine microstructure of Recent and Silurian chelicerates and the Cambrian arthropod *Sidneyia*: functional and evolutionary implications. *Arthropod Struct. Develop.* *47*, 12–24.
- Bicknell, R.D.C., Holmes, J.D., Edgecombe, G.D., Losso, S.R., Ortega-Hernández, J., Wroe, S., and Paterson, J.R. (2021a). Biomechanical analyses of Cambrian euarthropod limbs reveal their effectiveness in mastication and durophagy. *Proc. R. Soc. London B: Biol. Sci.* *288*, 20202075.
- Bicknell, R.D.C., Melzer, R.R., and Schmidt, M. (2021b). Three-dimensional kinematics of euchelicerate limbs uncover functional specialisation in eurypterid appendages. *Biol. J. Linn. Soc.* *135*, 174–183. <https://doi.org/10.1093/biolinnean/blab1108>.
- Bicknell, R.D.C., Smith, P.M., and Poschmann, M. (2020). Re-evaluating evidence of Australian eurypterids. *Gondwana Res.* *86*, 164–181.
- Braddy, S.J. (2001). Eurypterid palaeoecology: palaeobiological, ichnological and comparative evidence for a ‘mass–moult–mate’ hypothesis. *Palaeogeogr. Palaeoclimatol. Palaeoecol.* *172*, 115–132.
- Braddy, S.J., Poschmann, M., and Tetlie, O.E. (2008). Giant claw reveals the largest ever arthropod. *Biol. Lett.* *4*, 106–109.
- Brainerd, E.L., Gatesy, S.M., Baier, D.B., Hedrick, T.L., Metzger, K.A., Crisco, J., and Gilbert, S.L. (2010). X-ray reconstruction of moving morphology (XROMM): applications and accuracy in comparative biomechanics research. *J. Exp. Zool.* *313A*, 1–18.
- Bremer, O. (2017). Silurian vertebrates of Gotland (Sweden) and the Baltic Basin (Uppsala, Sweden): Doctoral thesis. Uppsala Universitet.
- Caster, K.E., and Kjellesvig-Waering, E.N. (1955). Untitled contribution. In *Treatise on Invertebrate Paleontology*, Størmer, L. Chelicerata., ed. (Geological Society of America and University of Kansas Press), p. P36.
- Caster, K.E., and Kjellesvig-Waering, E.N. (1964). Upper ordovician eurypterids of Ohio. *Palaeontograph. Americana* *4*, 297–358.
- Chlupáč, I. (1994). Pterygotid eurypterids (Arthropoda, Chelicerata) in the Silurian and Devonian of Bohemia. *J. Czech Geol. Soc.* *39*, 147–162.
- Collette, J.H., and Plotnick, R.E. (2020). Redescription, paleogeography, and experimental paleoecology of the Silurian phyllocarid *Gonatocaris*. *J. Paleontol.* *94*, 906–921.
- Dunlop, J.A., Penney, D., and Jekel, D. (2020). A Summary List of Fossil Spiders and Their Relatives. *World Spider Catalog Version 20.5* (Natural History Museum Bern).
- Esteve, J., Hughes, N.C., and Zamora, S. (2011). Purujosa trilobite assemblage and the evolution of trilobite enrollment. *Geology* *39*, 575–578.
- Esteve, J., Rubio, P., Zamora, S., and Rahman, I.A. (2017). Modeling enrolment in Cambrian trilobites. *Palaeontology* *60*, 423–432.
- Garwood, R., and Dunlop, J. (2014). The walking dead: Blender as a tool for paleontologists with a case study on extinct arachnids. *J. Paleontol.* *88*, 735–746.
- Garwood, R.J., Dunlop, J.A., Knecht, B.J., and Hegna, T.A. (2017). The phylogeny of fossil whip spiders. *BMC Evol. Biol.* *17*, 105.
- Gatesy, S.M., Baier, D.B., Jenkins, F.A., and Dial, K.P. (2010). Scientific rotoscoping: a morphology-based method of 3-D motion analysis and visualization. *J. Exp. Zool.* *313A*, 244–261.
- Gozalo, R., Liñán, E., and Dies Álvarez, M.E. (2003). Intraspecific dimorphism in an evolutionary series of paradoxidids from the middle Cambrian of Murero, Spain. *Spec. Pap. Palaeontol.* *70*, 141–156.
- Hanken, N.-M., and Størmer, L. (1975). The trail of a large Silurian eurypterid. *Fossils Strata* *4*, 255–270.
- Harvey, M.S. (2003). Catalogue of the Smaller Arachnid Orders of the World: Amblypygi, Uropygi, Schizomida, Palpigradi, Ricinulei and Solifugae (CSIRO Publishing Huntingdon).
- Holm, G. (1898). Ueber die Organisation des *Eurypterus fischeri* Eichwald. *Mem. Acad. Sci. Saint Petersburg* *8*, 1–57.
- Hughes, E.S., and Lamsdell, J.C. (2021). Discerning the diets of sweep-feeding eurypterids: assessing the importance of prey size to survivorship across the Late Devonian mass extinction in a phylogenetic context. *Paleobiology* *47*, 271–283.
- Kjellesvig-Waering, E.N. (1964). A synopsis of the Family Pterygotidae Clarke and Ruedemann, 1912 (Eurypterida). *J. Paleontol.* *38*, 331–361.
- Lamsdell, J.C., Briggs, D.E.G., Liu, H.P., Witzke, B.J., and McKay, R.M. (2015). The oldest described eurypterid: a giant Middle Ordovician (Darrivilian) megalograptid from the Winneshiek Lagerstätte of Iowa. *BMC Evol. Biol.* *15*, 169.
- Lamsdell, J.C., and Selden, P.A. (2017). From success to persistence: identifying an evolutionary regime shift in the diverse Paleozoic aquatic arthropod group Eurypterida, driven by the Devonian biotic crisis. *Evolution* *71*, 95–110.
- McArthur, I.W., Miranda, G.S., Seiter, M., and Chapin, K.J. (2018). Global patterns of sexual dimorphism in Amblypygi. *Zool. Anz.* *273*, 56–64.

- McLean, C.J., Garwood, R.J., and Brassey, C. (2019). Sexual dimorphism in the size and shape of the raptorial pedipalps of giant whip spiders (Arachnida: Amblypygi). *J. Zool.* **310**, 45–54.
- McCoy, V.E., Lamsdell, J.C., Poschmann, M., Anderson, R.P., and Briggs, D.E.G. (2015). All the better to see you with: eyes and claws reveal the evolution of divergent ecological roles in giant pterygotid eurypterids. *Biol. Lett.* **11**, 20150564.
- Meyer, D.L., and Davis, R.A. (2009). A Sea Without Fish: Life in the Ordovician Sea of the Cincinnati Region (Indiana University Press).
- Ortega-Hernández, J., Esteve, J., and Butterfield, N.J. (2013). Humble origins for a successful strategy: complete enrolment in early Cambrian olenellid trilobites. *Biol. Lett.* **9**, 0679.
- Plotnick, R.E. (1985). Lift based mechanisms for swimming in eurypterids and portunid crabs. *Trans. R. Soc. Edinb. Earth Sci.* **76**, 325–337.
- Plotnick, R.E., and Baumiller, T.K. (1988). The pterygotid telson as a biological rudder. *Lethaia* **21**, 13–27.
- Poschmann, M., Schoenemann, B., and McCoy, V.E. (2016). Telltale eyes: the lateral visual systems of Rhenish Lower Devonian eurypterids (Arthropoda, Chelicerata) and their palaeobiological implications. *Palaeontology* **59**, 295–304.
- Prendini, L., Weygoldt, P., and Wheeler, W.C. (2005). Systematics of the *Damon variegatus* group of African whip spiders (Chelicerata: Amblypygi): evidence from behaviour, morphology and DNA. *Organ. Divers. Evol.* **5**, 203–236.
- Ritchie, A. (1968). *Lanarkopterus dolichoschelus* (Størmer) gen. nov., a mixopterid eurypterid from the upper Silurian of the Lesmahagow and Hagshaw Hills inliers, Scotland. *Scott. J. Geol.* **4**, 317–338.
- Ruedemann, R. (1921). A recurrent Pittsford (Salina) fauna. *New York State Mus. Bull.* **219–20**, 205–215.
- Rudkin, D.M., Young, G.A., Elias, R.J., and Dobrzanski, E.P. (2003). The world's biggest trilobite—*Isotelus rex* new species from the upper Ordovician of northern Manitoba, Canada. *J. Paleontol.* **77**, 99–112.
- Santer, R.D., and Hebets, E.A. (2009). Prey capture by the whip spider *Phrynus marginemaculatus* C. L. Koch. *J. Arachnol.* **37**, 109–112.
- Schmidt, M., Hazerli, D., and Richter, S. (2020). Kinematics and morphology: a comparison of 3D patterns in the 5th pereopod of swimming and nonswimming crab species (Malacostraca, Decapoda, Brachyura). *J. Morphol.* **281**, 1547–1566.
- Schmidt, M., Liu, Y., Zhai, D., Hou, X.-G., and Melzer, R.R. (2021a). Moving legs: a workflow on how to generate a flexible endopod of the 518 million-year-old Chengjiang arthropod *Ercaicunia multinodosa* using 3D-kinematics (Cambrian, China). *Microsc. Res. Tech.* **84**, 695–704.
- Schmidt, M., Melzer, R.R., and Bicknell, R.D.C. (2021b). Kinematics of whip spider pedipalps: a 3D comparative morpho-functional approach. *Integr. Zool.* <https://doi.org/10.1111/1749-4877.12591>.
- Selden, P.A. (1981). Functional morphology of the prosoma of *Baltoeurypterus tetragonophthalmus* (Fischer) (Chelicerata: Eurypterida). *Trans. R. Soc. Edinb. Earth Sci.* **72**, 9–48.
- Selden, P.A. (1984). Autecology of Silurian eurypterids. *Spec. Pap. Palaeontol.* **32**, 39–54.
- Størmer, L. (1934). Merostomata from the Downtonian Sandstones of Ringerike, Norway. *Skrifter utgitt av Det Norske Videnskaps-akademi I Oslo. I. Matem.-Naturvid. Klasse* **10**, 1–125.
- Størmer, L., and Kjellesvig-Waering, E.N. (1969). Sexual dimorphism in eurypterids, p. 201–214. In *Sexual Dimorphism in Fossil Metazoa and Taxonomic Implications*, G.E.G. Westermann, ed. (International Union of Geological Sciences).
- Tollerton, V.P. (1989). Morphology, taxonomy, and classification of the order Eurypterida Burmeister, 1843. *J. Palaeontol.* **63**, 642–657.
- Waterston, C.D. (1964). Observations on pterygotid eurypterids. *Earth Environ. Sci. Trans. R. Soc. Edinb.* **66**, 9–33.
- Waterston, C.D. (1979). Problems of functional morphology and classification in stylonuroid eurypterids (Chelicerata, Merostomata), with observations on the Scottish Silurian Stylonuroidea. *Trans. R. Soc. Edinb.* **70**, 251–322.
- Waterston, C.D., Oelofsen, B.W., and Oosthuizen, R.D.F. (1985). *Cyrtoctenus wittebergensis* sp. nov. (Chelicerata: Eurypterida), a large sweep-feeder from the Carboniferous of South Africa. *Earth Environ. Sci. Trans. R. Soc. Edinb.* **76**, 339–358.
- Weygoldt, P. (1996). Evolutionary morphology of whip spiders: towards a phylogenetic system (Chelicerata: arachnida: Amblypygi). *J. Zoolog. Syst. Evol. Res.* **34**, 185–202.
- Weygoldt, P. (2000). Whip Spiders (Chelicerata: Amblypygi): Their Biology, Morphology and Systematics (Apollo Books).
- Weygoldt, P. (2002). Amblypygi. In *Amazonian Arachnida and Myriapoda*, J. Adis, ed. (Pensoft Publishers), pp. 293–302.
- Zahavi, A. (1975). Mate selection: a selection for a handicap. *J. Theor. Biol.* **53**, 205–214.

STAR★METHODS

KEY RESOURCES TABLE

REAGENT or RESOURCE	SOURCE	IDENTIFIER
Experimental models: Organisms/strains		
<i>Damon medius</i>	Bavarian State Collection of Zoology (ZSMA)	ZSMA19730285
<i>Heterophrynus elaphus</i>	Bavarian State Collection of Zoology (ZSMA)	ZSMA20120286
Software and algorithms		
Blender	www.blender.org	2.9
Maya	www.autodesk.com	2020
Mimics	www.materialise.com	23.0

RESOURCE AVAILABILITY

Lead contact

Further information and requests for resources and reagents should be directed to and will be fulfilled by the Lead Contact, Michel Schmidt (m.schmidt30@outlook.de).

Materials availability

This study did not generate new unique reagents.

Data and code availability

All data reported in this paper will be shared by the lead contact upon request.

This paper does not report original code.

Any additional information required to reanalyze the data reported in this paper is available from the lead contact upon request.

EXPERIMENTAL MODELS AND SUBJECT DETAILS

The following whip spider species were analyzed: *Damon medius*: male, 28 mm body size, adult, preserved in 75 % EtOH, collected in 1973 in Cameroon by Roewer, collection number ZSMA19730285. *Heterophrynus elaphus*: female, 33 mm body size, adult, preserved in 75% EtOH, collected in 2012 in Peru by Diller, collection number ZSMA20120286. They are stored at the Bavarian State Collection of Zoology (ZSMA), Bavaria, Munich, Germany.

METHOD DETAILS

Modern analogs

Whip spider specimens from *Damon medius* and *Heterophrynus elaphus* were recently analyzed (Schmidt et al., 2021b). The specimens were scanned with a Phoenix Nanotom microcomputed tomography scanner housed at the Bavarian State Collection of Zoology using the following scanning parameters: 90 kV, 110 mA, 2359 TIFFs, voxel size 15. Surface rendering was performed using Mimics version 23.0 (Materialise, Leuven, Belgium) to generate pedipalp surface models. Those were segmented using the 'Segmenting' tool. Surface models were then exported as .obj files for import into Autodesk Maya 2020 (Autodesk, San Rafael, USA) for kinematic analyses of the range of motion (see below).

3D reconstructions of eurypterids and prey

Megalograptus and *Mixopterus* are known from multiple species (Dunlop et al., 2020). As such, we selected *Me. ohioensis* and *Mi. kiaeri* as the most well-documented taxa within the genera with the most complete fossils specimens and morphological drawings (Caster and Kjellesvig-Waering, 1964; Størmer, 1934). The models were created in Blender 2.9 using the sculpting tool (Garwood and Dunlop, 2014). *Megalograptus ohioensis* 3D models were constructed using data in Caster and Kjellesvig-Waering (1964): prosoma was

modeled after text Figure 1 (description p. 316–318); the Appendage II models were based on text Figures 5 and 6 (description p. 319–321); the Appendage III models were based on text Figures 7 and 8 (description p. 321–324). Conversely, *Mixopterus kiaeri* 3D models were based on the data in Størmer (1934, Figures 13 and 14, plates 5–7; description p. 106–109). Original drawings and new photographs of *Megalograptus ohioensis* and *Mixopterus kiaeri* are shown in Figure S9. Proposed prey items are based on taxa known to co-occur with the eurypterids. The anaspid fish model was based on Bremer (2017), the trilobite was based on Rudkin et al. (2003).

It is important to note that *Me. ohioensis* Appendages II and III are more well documented and pictured in delicate detail than appendages of *Mi. kiaeri*. However, this did not impact our ability to present reconstructions. Furthermore, the complete spine length on podomere 3 of the *Me. ohioensis* Appendage III is unknown (Caster and Kjellesvig-Waering, 1964, p. 323). As such, we present a minimal estimate of size. All measurements and ratios of the 3D models were calculated using width and length of the prosoma of the *Me. ohioensis* (Cincinnati Museum Center IP 24119A; Caster and Kjellesvig-Waering, 1964, p. 317) and *Mi. kiaeri* (Paleontological Museum, Oslo H 2044; Størmer, 1934, p. 115) holotypes. Inflation of the podomeres and the prosoma was set to a reasonable, comprehensible value.

The angle between the two longest spines in *Megalograptus ohioensis* (Figures 1D, S2E, and S2F) is based on our interpretation—and was modeled kinematically to allow distal podomeres to pass through them. A smaller angle would have prevented adduction.

Kinematic marionettes

Kinematic deflection was performed using Autodesk Maya 2021 following steps in Schmidt et al. (2021a, Figures 1–3):

Three-dimensional models were exported from Blender as .obj files and imported into Maya. Then, hypothetical joint axes were constructed as simple cylinders being the mathematically most natural form. All eurypterid joints were considered as bicondylar, being the most expressed joint type in modern arthropods. The hypothetical joint axes were then placed inside each bicondylar joint fitting the condyles, that is combining both articulation points. Artificial joints (shaped as spheres), so-called *srjoints* were created using the X_ROOM add-on in Maya (following Gatesy et al., 2010; Brainerd et al., 2010) by typing *joint* in the MEL line in Maya. After assigning those *srjoints* to each bicondylar joint and hence joint axis using commands *point constrain* and *orient constrain*, each joint was rotatable alongside its axis, thus rotation being independent of the world coordinate system. Hereafter, each distal joint was subordinated to its adjacent proximal one (Schmidt et al., 2021a, Figure 3.28) to ultimately create a kinematic marionette. Here, a displacement of proximal podomeres resulted in distal podomeres following this movement. We modeled all podomeres except one as moving in horizontal plane. Joint 2 in *Megalograptus ohioensis*, the podomere 2-podomere 3 joint (Caster and Kjellesvig-Waering 1964, p. 321; our Figures 1C and S2) was an exception. Due to podomere morphology and position of hypothetical joint axes, this joint was allowed to move within the vertical plane, resulting in appendage elevation and depression.

ROM analyses

The maximum excursion angle measurement of each joint, ROM, was performed in Autodesk Maya 2021. We refer to this as range of motion (ROM) solely (compare Schmidt et al., 2021b). However, when obtaining data on maximum excursion angles in each joint and the total scope of possible movements regarding a Cartesian coordinate system, we usually differ between single range of motion (sROM) and total range of motion (tROM; see Schmidt et al., 2020, our Table S2). Here, each joint (a proximal podomere, a distal podomere, and a joint axis) was placed within a unique coordinate system. Both podomeres were subordinated to the joint axis, after which the model was placed inside the vertical axis. At this point, rotation in the z-axis was observed. Maximum range of motion was considered when podomeres (or spines) collided.

Movement directions

For the movement of the appendages, we use the terms abduction (movement away from the midline of the body) and adduction (movement towards the midline of the body). All joints but joint 2 (= podomere 2-podomere 3 joint) in the *Megalograptus ohioensis* Appendage III work in those two directions. Joint 2 fulfills a dorso-ventral movement (Caster and Kjellesvig-Waering 1964, p. 321). This movement, therefore,

is regarded as elevation (movement in a superior direction) and depression (movement in an inferior direction).

Spines

Spinosity of *Megalograptus ohioensis* and *Mixopterus kiaeri* appendages could impact flexibility and range of motion. The spines were likely socketed outgrowths from the appendage cuticle. While we consider them non-mobile, we cannot be certain the spines were totally rigid. Indeed, whether spines could react to distally applied pressure or if they were completely rigid would impact the kinematic analyses and the range of motion. As we modelled the spines as rigid, when a spine contacted another appendage section, movement ended. This may have resulted in an underestimation of podomere range of motion—sea scorpion appendages may have been more flexible than we have proposed.

Literature is divided when it comes to that question with some (*Megalograptus*: [Caster and Kjellesvig-Waering, 1964](#), pp. 320, 325) differing movable and immovable spines, while others (*Mixopterus*: [Størmer, 1934](#), p. 109) only speak of immovable. [Ritchie \(1968, p. 326\)](#) who erected the genus *Lanarkopterus* for a former member of *Mixopterus* also differed between movable socketed spines and immovable.

In our modern whip spider analogs, all spines are cuticular outgrowths and thus immovable as well.

Terminology

Consider [Table S3](#) for definitions of words used here. [Størmer \(1934\)](#) and [Caster and Kjellesvig-Waering \(1964\)](#) used 'joint' to describe podomeres—single appendage units. Here, joint refers to a flexible construction linking two adjacent podomeres. The authors furthermore referred to as coxa, joint 1, joint 2, etc. We count—for a more comprehensive understanding—the coxa as podomere 1, followed by podomere 2, podomere 3, etc. Both, [Størmer \(1934\)](#) and [Caster and Kjellesvig-Waering \(1964\)](#) considered terminal spines on Appendages II and III single podomeres (joints). Here, we consider them as spinous developments from their adjacent podomeres. Hence, our Appendage II and III podomere counts are one less than in the original publications. This did not impact the kinematic analyses.

QUANTIFICATION AND STATISTICAL ANALYSES

All the relevant analyses were reported in the relevant sections above in the [STAR Methods](#).